J Korean Soc Radiol 2009 ; 61 : 17-22

Warthin's Tumor of the Parotid Gland:
CT and MR Features[1]

Yun Hee Lee, M.D., In Kyu Yu, M.D., Moon Hee Han, M.D.[2], Byung-Hee Lee, M.D., Min Sun Kim, M.D., Chang Joon Song, M.D.[3]

Purpose: In this study, we have evaluated the imaging features of Warthin's tumor of the parotid gland with the use of CT and MR imaging.

Materials and Methods: CT (n = 30) and MR (n = 7) images of 26 patients (M:F=23:3; age range, 38-76 years; mean age, 58 years) with surgically-proven Warthin's tumor (n = 37) were reviewed with a focus on bilaterality, multiplicity, location, size, demarcation, margin, enhancement pattern and MR signal intensity.

Results: Lesions were bilateral in seven patients (27%), multiple in nine patients (35%) and unilateral multiple in four patients (15%). Tumors were located in the superficial lobe (65%), deep lobe (24%) and both lobes (11%) of the parotid gland. Most tumors had a clear (95%) and smooth margin (95%) with a round or oval shape. Tumors mainly showed a solid and cystic composition (n = 24, 65%) and all solid stroma showed poor or weak enhancement on both CT and MR images. Papillary projections from the peripheral wall were clearly seen (n = 6, 86%).

Conclusion: Warthin's tumor is frequently seen in the parotid superficial lobe of older males with a higher bilateral and multiple tendency. Warthin's tumor shows cystic portions with papillary projections at the wall on CT images and focal high signal intensity (SI) on T1-weighted images with dense nodular enhancement on MR images.

Index words : Salivary glands
Adenolymphoma
Parotid gland
Parotid neoplasms
Magnetic resonance (MR)
Tomography, X-ray computed

[1]Department of Radiology, Eulji University Hospital, Daejeon, Korea
[2]Department of Radiology, Seoul National University Hospital, Seoul, Korea
[3]Department of Radiology, Chungnam National University Hospital, Daejeon, Korea
This study was presented at the 20th Annual Meeting of European Society of Head and Neck Radiology (ESHNR) in Oslo, Norway 2007.
Received January 29, 2009 ; Accepted March 24, 2009
Address reprint requests to : In Kyu Yu, M.D., Department of Radiology, Eulji University Hospital
Dunsan 2-dong, Seo-gu, Daejeon 302-799, Korea.
Tel. 82-42-611-3562 Fax. 82-42-611-3590 E-mail: midosyu@eulji.ac.kr

Warthin's tumor (adenolymphoma or papillary cystadenoma lymphomatosum) is the second most common benign tumor of the parotid gland, representing approximately 2% to 10% of all parotid tumors (1–3, 6–8). The lesion is almost exclusively limited to the parotid gland and frequently has bilateral and multifocal unilateral involvement. Warthin's tumor is also known to have a greater tendency to undergo gross cystic change (4–5, 9). However, the imaging features of Warthin's tumor have not been well documented in a large series. In this study, we have evaluated the imaging features of Warthin's tumor of the parotid gland with the use of CT and MR imaging.

Materials and Methods

In this study, CT and MR images of surgically proven 37 Warthin's tumors in 26 patients were included. We evaluated CT images of 30 Warthin's tumors in 22 patients and MR images of seven Warthin's tumors in four patients. The patient age ranged from 38 to 76 years (mean age, 58 years) and there was a striking male predominance (M: F = 23:3). We evaluated the imaging features with attention focused on bilaterality, multiplicity, location, size, demarcation and shape of the tumor margin, tumor composition, presence of papillary projections from the wall, signal intensity of the tumor on MR images and enhancement features. Tumor composition was classified into three types: an entirely cystic mass with a peripheral solid enhancing rim (type 1), a solid and cystic mass (type 2), a solid mass with a large cystic portion (type 2A), a mainly solid mass with small cysts (type 2B) and an entirely solid enhancing mass (type 3) (Fig. 2). We evaluated enhancement features of both solid stroma and cystic portions of tumors. The study was approved by our institutional review board. All patients gave written informed consent.

Results

Lesions were bilateral in seven patients (27%), multiple in nine patients (35%) and unilateral multiple in four patients (15%) (Fig. 1). Tumors were located in the superficial lobe (65%), deep lobe (24%) and both lobes (11%) of the parotid gland (Figs. 1–4). Tumors ranged in size from 1.0 cm to 6.0 cm (mean, 2.8 cm). Most tumors had a clear (95%) and smooth margin (95%) with a round or oval shape. As seen on post-contrast images, tumors showed mainly a solid and cystic composition (type 2, n = 24, 65%) (Fig. 1B, C) or were seen as entirely cystic lesions (type 1, n = 7, 19%) (Figs. 2A, 3A) and as entirely solid lesions (type 3, n = 6, 16%) (Fig. 1D). Of the tumors 84% showed cystic portions. Tumors showed a tendency for more frequent cystic change according to an increased

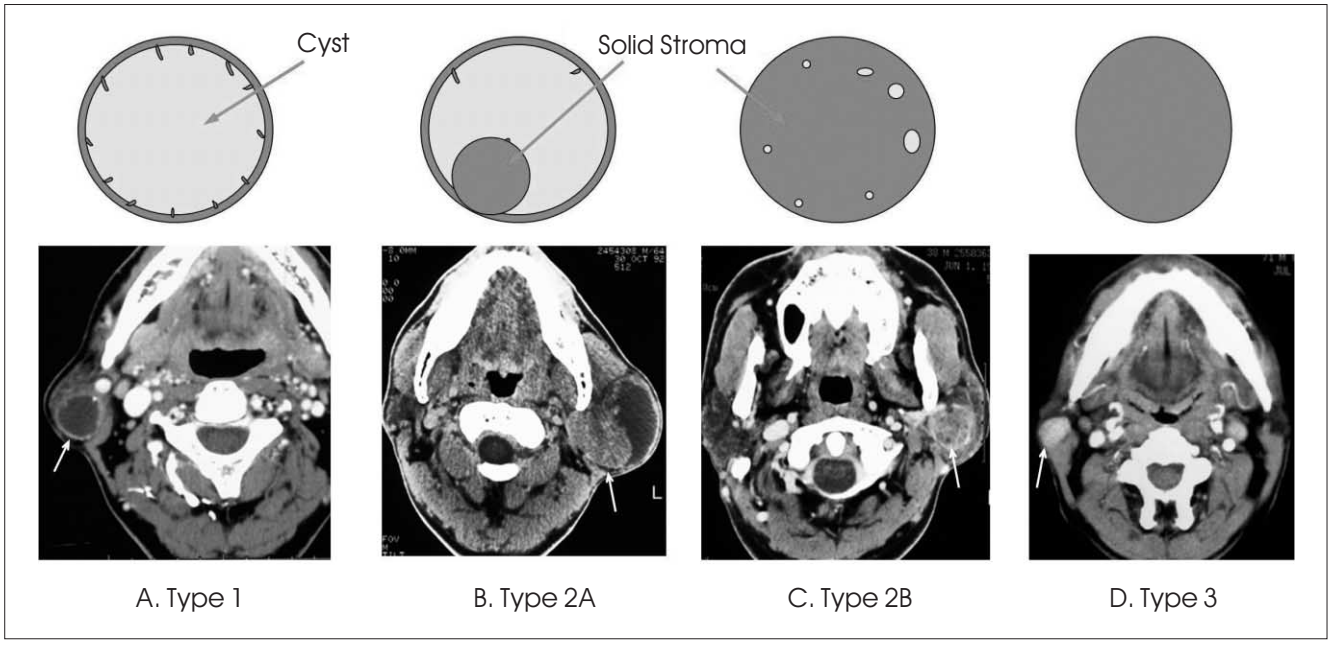

Fig. 1. Classification of the shape of Warthin's tumor is presented.
Type 1 tumors are entirely cystic masses (arrow) with a peripheral solid enhancing rim (A). Type 2 tumors are solid and cystic masses; a solid mass with a large cystic portion (type 2A, arrow) (B) and a mainly solid mass with small cysts (type 2B, arrow) (C). Type 3 tumors are entirely solid enhancing masses (arrow) (D).

size (62% of tumors less than 2 cm in diameter and 96% of tumors greater than 2 cm in diameter) (Table 1). Of the lesions, 83% of the tumors with no visible cystic portions were smaller than 2 cm in diameter. Papillary projections from the peripheral wall were clearly seen in most type 1 tumors (n = 6, 86%) (Fig. 2) but were not seen for type 2 and type 3 tumors. All solid stroma of tumors showed poor or weak enhancement on both CT and MR images (Fig. 1). On delayed coronal CT images (n = 12), the cystic portion showed slightly decreased (50%) or increased (42%) attenuation as compared with the attenuation on early axial images.

All solid stroma of tumors showed low or intermediate signal intensity (SI), but were slightly hyperintense as compared to muscle on T1-weighted images (T1WI) and showed intermediate or slightly heterogeneous SI on T2-weighted images (T2WI) and showed weak solid enhancement. All lesions were comprised of cystic portions with focal hyperintense or slightly hyperintense SI portions on T1WI and these portions showed variable SI on T2WI-high SI for four lesions, low or intermediate SI for three lesions and paradoxically decreased SI after gadolinium enhancement (Figs. 3 and 4). On post-contrast MR images, there was focal nodular solid enhancement seen for the peripheral wall of the tumor for six lesions (86%); four lesions showed definite enhancement and two lesions showed faint enhancement (Fig. 4).

Table 1. Tumor Composition according to Tumor Size

	< 2 cm	2–4 cm	> 4 cm	Total
Type 1	1 (8%)	6 (27%)	–	7 (19%)
Type 2A	7 (54%)	10 (45%)	2 (100%)	19 (54%)
2B	–	5 (23%)	–	5 (11%)
Type 3	5 (38%)	1 (5%)	–	6 (16%)
Total	13	22	2	37 (100%)

Discussion

The most likely pathogenesis of Warthin's tumor is adenomatous epithelial proliferation from embryologic entrapment of heterotopic salivary gland ductal epithelial tissue within intraparotid and periparotid lymph

Fig. 2. Features of type 1 tumors with papillary projections are shown.
A. An entirely cystic mass is well visualized in the posterior superficial lobe of the right parotid gland with multiple numerous papillary projections at the wall (arrows). The cystic contents show slightly increased attenuation.
B. Another type 1 tumor shows prominent multiple papillary projections at the wall (arrows).
C. A comparison case of a cystic pleomorphic adenoma shows no papillary projections at the tumor wall (arrows).
D. Microscopic findings of the papillary projections show epithelial tissue (arrows) composed of double-layers of oncocytes (H & E staining, ×40).

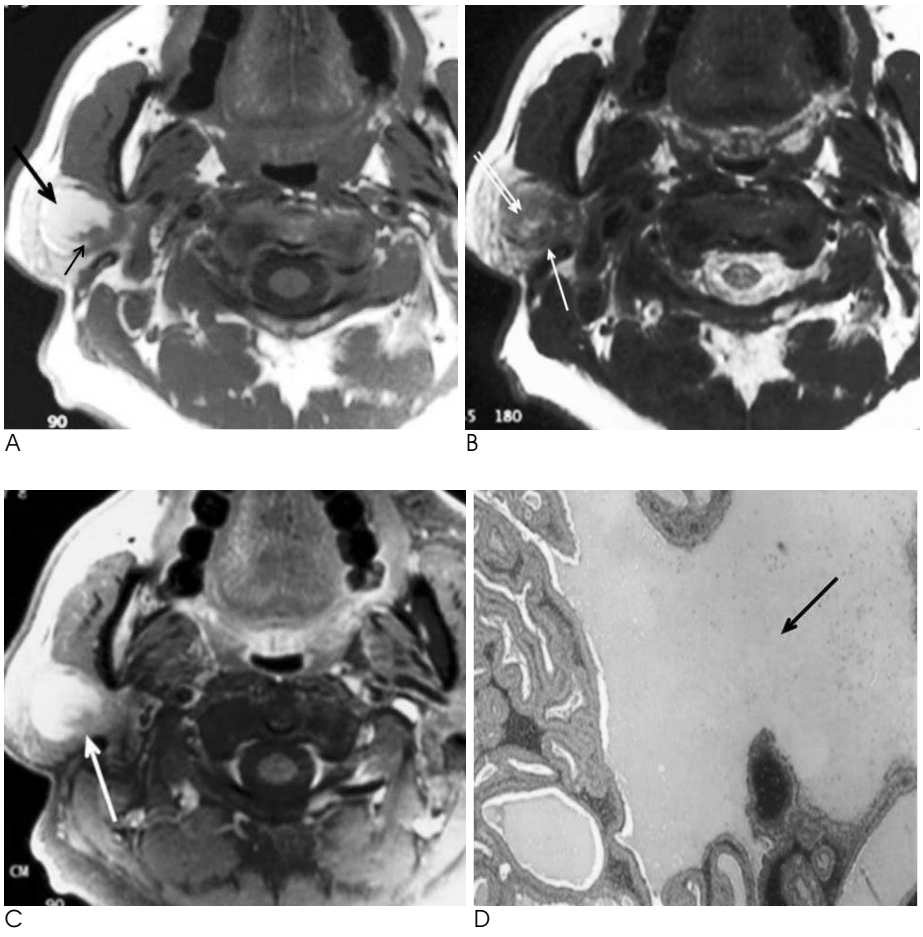

Fig. 3. Imaging features of a type 2A tumor in the right parotid gland are shown.
A. Hypointense solid stroma (arrow) with a large hyperintense cystic portion (large arrow) is seen on a T1-weighted image.
B. On a T2-weighted image, the solid stroma show low signal intensity (arrow) while the cystic portion (double arrow) shows intermediate signal intensity
C. After gadolinium enhancement, the solid stroma shows faint enhancement (arrow).
D. As seen from the microscopic findings, the cystic space (arrow) is well visualized with peripheral solid epithelial portions (H & E staining, ×40).

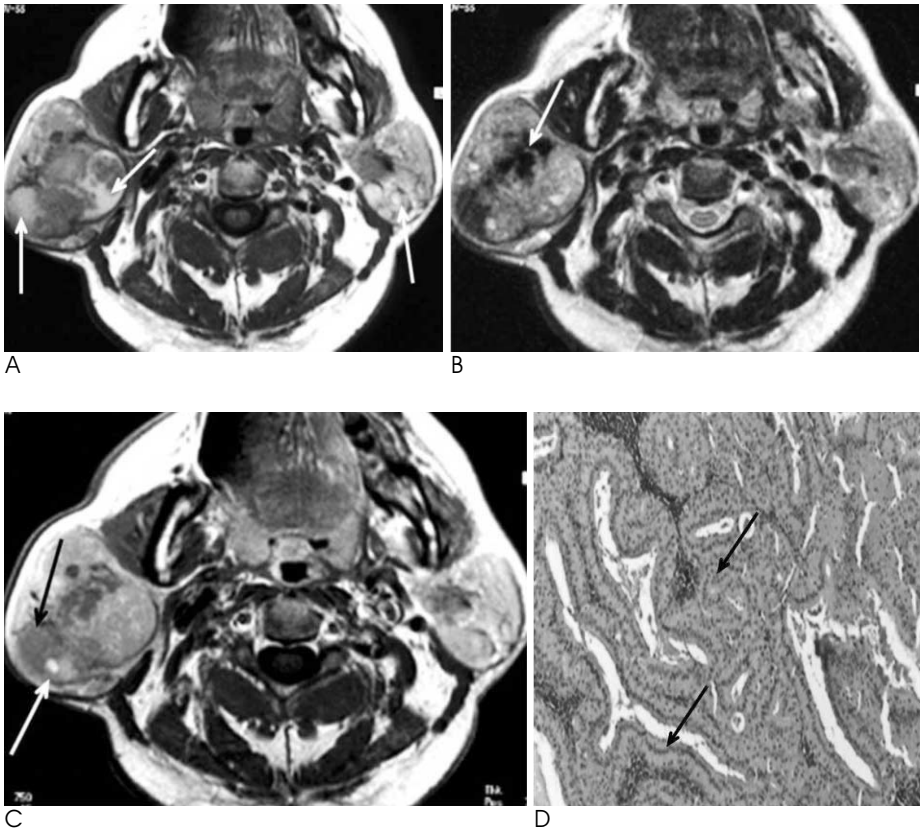

Fig. 4. Imaging features of type 2B tumors in both parotid glands are shown.
A. Multifocal hyperintense small cysts (arrow) with solid stroma in both parotid glands on a T1-weighted image are seen.
B. On a T2-weighted image, a prominent low signal intensity portion (arrow) is seen, which is suggestive of hemorrhagic foci.
C. After gadolinium enhancement, focal dense nodular enhancement (white arrow) is well visualized. The solid stroma show faint enhancement and the cystic space show decreased signal intensity (arrow).
D. As seen from the microscopic findings, compact solid epithelial tissue (arrows) composed of a double layer of oncocytes is visualized (H & E staining, ×100).

nodes (1-2, 6-7). Microscopically, these tumors have a double layer of oncocytes that line the papillary projections, which characteristically extend into the cystic spaces (3, 8). These oncocytes have a large number of mitochondria, and these cells most often accumulate technetium-99m pertechnetate as seen on radionuclide scans. The unknown stimulus that leads to the development of this tumor can apparently act on any such epithelial nodal inclusions, and thus there is the possibility for the development of multiple tumors. Although this tumor has known to be bilateral in 10% and multiple in 15% of cases, careful microscopic examinations of pathology specimens have suggested that multifocality is present in almost 30% of specimens (4, 9). Our series showed a higher incidence of bilaterality and multiplicity as compared to previous reports, that is, bilaterality in 27% of cases and multiplicity in 35% of cases. This difference is probably due to the higher resolution of recent imaging modalities. Grossly, the tumor is seen as ovoid, thin encapsulated and either cystic or semisolid (4, 9).

Most tumors show a benign-looking appearance in the superficial lobe of the parotid gland, with the tumors clear and smooth marginated. In our series, most tumors appeared solid and had cystic heterogeneous contents in approximately two-thirds of the lesions. The tumors were seen as an entirely cystic mass with a peripheral solid stromal rim for approximately one-fifth of the lesions and as an entirely solid mass for approximately one-sixth of the lesions. These tumors showed cystic portions more frequently according to an increased size. Cystic portions were seen in 62% of tumors less than 2 cm in diameter and were seen in 96% of tumors greater than 2 cm in diameter. For tumors less than 2 cm in diameter, almost 40% of the tumors appeared as an entirely solid mass with no detectable cystic portions. Most tumors (84%) showed some discernible cystic portions in our series. Most type 1 tumors showed small multiple papillary projections at the peripheral wall, which correspond to epithelial and lymphoid stroma, and the projections seem to be a feature of Warthin's tumor on CT images rather than for a cystic pleomorphic adenoma. All solid stroma showed poor or weak enhancement on both CT and MR images. It was interesting that the cystic contents of tumors showed slightly increased or decreased attenuation on delayed coronal CT images or decreased SI on MR images according to the scan time after contrast enhancement. This effect seemed due to the diffusion of contrast material from the wall to the cystic spaces (4, 10-11).

On MR images, tumor demarcation and contents were more clearly seen. Intermediate SI of the stroma seen on both T1WI and T2WI was attributed to the presence of high cellular epithelial components, while high or heterogeneous SI of the stroma seen on T2WI was due to the presence of mixed epithelial tissue with lymphoid proliferation and cyst formation as identified on pathological examinations (4). Focal hyperintense areas seen on T1WI correspond to semisolid cysts that contain proteinaceous fluids with cholesterol crystals (5). In the differential diagnosis of parotid lesions with high SI seen on T1WI, hemorrhage in a tumor such as a pleomorphic adenoma, hemangioma, malignant tumor and high proteinaceous contents such as an abscess should be considered, but other combined features such as the shape of the cyst with MR SI can be useful for the differentiation. For the differentiation of a mass with low SI as seen on T2WI, a high cellular malignant tumor, hemorrhage, fibrosis and high proteinaceous contents should be included (5-10). Dense nodular enhancement at the peripheral stroma, as seen in most MR cases (6/7), seems to be attributed to the presence of mitochondria-rich oncocytes, as seen for a technetium-99m scan (11) and this finding can be a another clue for the presence of Warthin's tumor on MR images.

In summary, Warthin's tumor is frequently seen in the parotid superficial lobe of older male patients with higher bilateral and multiple tendency. On CT images, the tumor appears as a benign-looking smooth, well-marginated, mostly solid and cystic mass (in two-thirds of cases) or as an entirely cystic mass with peripheral papillary projections (in one-fifth of cases) and as an entirely solid mass with a size of less than 2 cm in diameter. On MR images, most solid stromal components show intermediate SI with focal nodular enhancement, and semisolid cystic contents show high SI on T1WI.

In conclusion, Warthin's tumor shows cystic portions with papillary projections at the wall on CT images and focal high SI is seen on TIWI with dense nodular enhancement on MR images.

References

1. Minami M, Tanioka H, Oyama K, Itai Y, Eguchi M, Yoshikawa K, et al. Warthin tumor of the parotid gland: MR- pathologic correlation. *AJNR Am J Neuroradiol* 1993;14:209-214
2. Swartz JD, Rothman MI, Marlowe FI, Berger AS. MR imaging of parotid mass lesions: attempts at histopathologic differentiation. *J Comput Assist Tomogr* 1989;13:789-796

3. Schlakman BN, Yousem DM. MR of intraparotid mass. *AJNR Am J Neuroradiol* 1993;14:1173-1180
4. Joe VQ, Westesson PL. Tumors of parotid gland: MR imaging characteristics of various histologic types. *AJR Am J Roentegnol* 1994;163:433-438
5. Ikeda M, Motoori K, Hanazawa T, Nagai Y, Yamamoto S, Ueda T, et al. Warthin tumor of the parotid gland: diagnostic value of MR imaging with histopathologic correlation. *AJNR Am J Neuroradiol* 2004;25:1256-1262
6. Batsakis JG, el-Naggar AK. Warthin's tumor. *Ann Otol Rhinol Laryngol* 1990;99:588-591
7. Aguirre JM, Echebarría MA, Martínez-Conde R, Rodriguez C, Burgos JJ, Rivera JM. Warthin tumor. A new hypothesis concerning its development. *Oral Surg Oral Med Oral Pathol Oral Radiol Endod* 1998;85:60-63
8. Hwang BT, Sugihara K, Kawashima K, Yamashita S. Scanning electron microscopic study of Warthin's tumor. *J Oral Pathol* 1987;16:118-123
9. Eveson JW, Cawson RA. Warthin's tumor (cystadenolymphoma) of salivary glands. A clinicopathologic investigation of 278 cases. *Oral Surg Oral Med Oral Pathol* 1986;61:256-262
10. Ikarashi F, Nakano Y, Nonomura N, Kawana M. Radiological findings of adenolymphoma (Warthin's tumor). *Auris Nasus Larynx* 1997;24:405-409
11. Park J, Inoue S, Ishizuka Y, Shindo H, Kawanishi M, Kakizaki D, et al. Salivary gland masses:dynamic MR imaging and pathologic correlation. *Nippon Igaku Hoshasen Gakkai Zasshi* 1997;57:581-585

대한영상의학회지 2009 ; 61 : 17-22

이하선의 Warthin 종양: CT 및 MR 소견[1]

[1]을지대학교 의과대학 을지대학병원 영상의학과
[2]서울대학교 의과대학 서울대학교병원 영상의학과
[3]충남대학교 의과대학 충남대학교병원 영상의학과

이윤희 · 유인규 · 한문희[2] · 이병희 · 김민선 · 송창준[3]

목적: 이하선에 발생하는 Warthin 씨 종양이 CT와 MR에서 어떤 영상학적 특징을 보이는지 알아보았다.
대상과 방법: 수술로 이하선의 Warthin 종양으로 확진된 환자 26명(M: F=23:3, 연령: 38-76 세, 평균=58세), 37개의 종양에서 CT(n=30) 및 MR(n=7) 소견을 후향적으로 분석하였다. 분석내용은 종양의 위치, 크기, 경계구분, 경계모양, 신호강도, 조영증강 형태이다.
결과: 양측성 병변 7명(27%), 다발성 병변 9명(35%), 그리고 한쪽 이하선에만 다발성 병변인 환자가 4명이었다(15%). 종양의 위치는 이하선의 천엽(65%)이 심엽(24%)보다 많았다. 종양 대부분은 원형 또는 타원형의 모양에, 경계가 확실히 구분되었고(95%), 95%에서 매끄러운 경계를 보였다. 또한, 낭성 및 고형성인 경우 (n=24, 65%)가 대부분이었으며, 종양의 모든 고형기질은 거의 조영증강이 안되거나, 약한 조영증강을 보였다. MR에서 종양의 모든 고형기질은 낮은 또는 중간의 신호강도를 보였으며, 조영증강 후 MR 영상에서는, 6개(86%)의 종양에서 주변부 외막에 결절성 조영증강을 보였다.
결론: Warthin 종양은 장, 노년남자에서 잘 생기고, 이하선의 주로 표층부에 있고 거의 경계가 분명하게 보인다. 영상학적으로 Warthin 종양은 CT에서 낭성 성분과 주변부 외막에 결절성 조영증강이 관찰되고, MR의 T1WI에서 중간신호강도와 결절성 조영증강을 보인다.